Journal of Materials Chemistry A

A Core-shell Cathode Substrate for Developing High-loading, High-performance Lithium-sulfur Batteries

Journal:	*Journal of Materials Chemistry A*
Manuscript ID	TA-ART-09-2018-009059.R2
Article Type:	Paper
Date Submitted by the Author:	20-Nov-2018
Complete List of Authors:	Yu, Ran; University of Texas at Austin, Materials Science and Engineering Chung, Sheng-Heng; University of Texas at Austin, Materials Science and Engineering Chen, Chunhua; Univ Sci tech of China, MSE Manthiram, Arumugam; University of Texas at Austin, Materials Science and Engineering

SCHOLARONE™
Manuscripts

Journal Name

ARTICLE

A Core-shell Cathode Substrate for Developing High-loading, High-performance Lithium-sulfur Batteries

Received 00th January 20xx,
Accepted 00th January 20xx

DOI: 10.1039/x0xx00000x

www.rsc.org/

Ran Yu,[a,b] Sheng-Heng Chung,[a] Chun-Hua Chen,*[,b] and Arumugam Manthiram*[,a]

Lithium-sulfur batteries with a high theoretical energy density would be a promising next-generation energy-storage system if their cell-fabrication parameters (*e.g.*, sulfur loading/content and the electrolyte/sulfur ratio) are improved to a practically necessary level. Herein, we report the design of a three-dimensional core-shell carbon substrate,integrating a porous internal core with a conductive external carbon nanofiber shell. Such a carbon substrate encapsulates a high amount of sulfur as the active material core to form a high-loading core-shell cathode, attaining an ultra-high sulfur loading and content of, respectively, 23 mg cm^{-2} and 75 wt.%. With distinguishable internal and external regions, the carbon substrate facilitates the redox reactions and hinders the polysulfide diffusion. Thus, the core-shell cathodes exhibit a high areal capacity and energy density of, respectively, 14 mA h cm^{-2} and 27 mW h cm^{-2} during cycling. During resting, they achieve a long shelf-life of one month with a low capacity-fade rate of 0.25% per day.

Introduction

Lithium-sulfur batteries are one of the most promising next-generation rechargeable systems because sulfur is an earth-abundant element with a high theoretical capacity of 1,672 mA h g^{-1}.[1] In order to bring the lithium-sulfur technology into the future battery market, current development focuses on reducing the intrinsic materials problems, such as the low conductivity of sulfur and the fast polysulfide diffusion. Recently, major research is devoted to ameliorating the extrinsic cell-fabrication parameters to realize a sufficient amount of sulfur and lean electrolyte in a cell.[2,3]

The intrinsic material problem is an inevitable consequence of the multiple-phase transitions of sulfur during cycling.[2,4] The phase transitions among solid-state sulfur, liquid-state polysulfides, and solid-state lithium sulfides lead the cathode to suffer continuous volume changes of about 80%.[5] The insulating nature of the solid-state sulfur and lithium sulfides causes a low electrochemical effectiveness of the cathode.[1,4] Moreover, polysulfides are highly soluble in the electrolyte. The dissolved polysulfides tend to diffuse out of the cathode and migrate toward the lithium-metal anode.[1,4-6]Consequently, the sulfur cathode and the lithium-metal counter electrode suffer from, respectively, the active material loss and the polysulfide contamination. The irreversible polysulfide relocation results in a fast capacity fade.[6] In order to improve the electrochemical performance of lithium-sulfur cells, various methods have been tried, among which the fabrication of nanocomposite with a core-shell structure is proved to be effective. Generally, the active material is encapsulated in various functional shells to form the core-shell nanocomposite.[7-16] The shells, such as polymers,[7-10] carbon-based materials,[11-15] and metal oxides,[16] provide strong physical and chemical confinements to polysulfides. The conductive shells also provide electron pathways to promote the redox reactions.[13,14]

However, all the intrinsic materials problems would be amplified when a cell has a high amount of sulfur and low electrolyte volume.[17,18] The assembly of cells with necessary cell-fabrication parameters has proven to cause several emerging extrinsic problems, including sluggish reaction kinetics, aggressive polysulfide migration, and poor discharge/charge efficiency.[2] These negative impacts make it difficult to achieve satisfactory cell performances. Despite full of challenges, a sufficient amount of sulfur at a low electrolyte/sulfur (E/S) ratio is the key to design practical lithium-sulfur batteries.[3] For this purpose, cathode substrates with a three-dimensional architecture have been evidenced as an effective method to host a sufficient amount of active material while keeping a reasonably high amount of sulfur utilization and cyclability.[2,3,17-21]

[a] *Materials Science and Engineering Program & Texas Materials Institute, The University of Texas at Austin, Austin, Texas 78712, United States.*
[b] *CAS Key Laboratory of Materials for Energy Conversions, Department of Materials Science and Engineering & Collaborative Innovation Center of Suzhou Nano Science and Technology, University of Science and Technology of China, Anhui Hefei 230026, China*

Electronic Supplementary Information (ESI) available: [microstructure analysis, dynamic battery characteristics, and a table summarizing electrochemical performances of lithium-sulfur cathodes in recent reports.See DOI: 10.1039/x0xx00000x

This journal is © The Royal Society of Chemistry 20xx

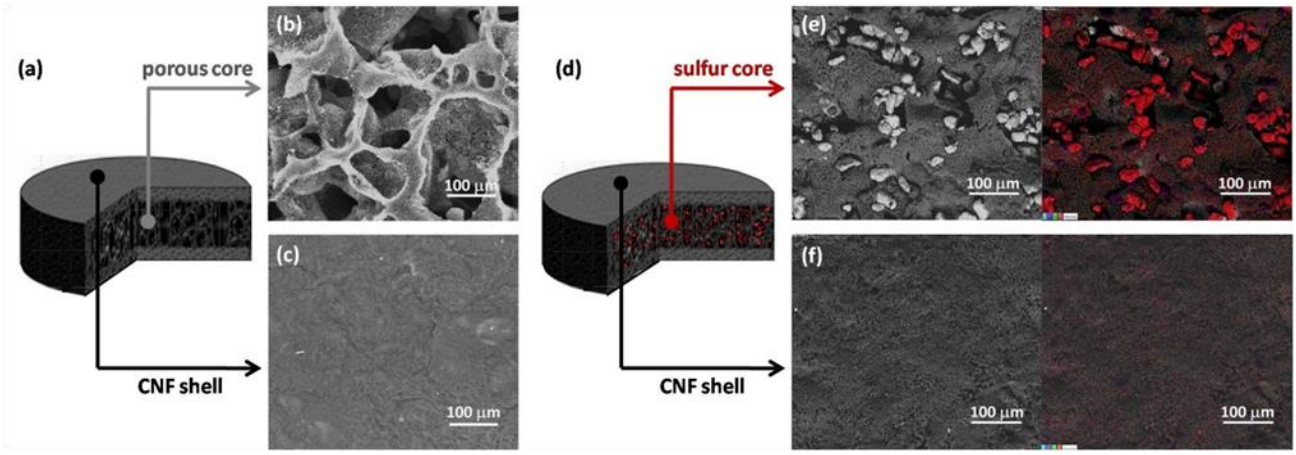

Fig. 1. (a) Illustration of the core-shell CNF substrate. Microstructural analysis of the substrate observed from (b) internal and (c) external

In this work, we design a three-dimensional core-shell cathode substrate that possesses a porous internal core region to accommodate and absorb a high amount of active material (23.0 mg cm^{-2} and 75 wt.% sulfur). Surrounding the core, a relatively dense external carbon shell limits the loss of active material and offers a conductive network. Therefore, the cells fabricated with the core-shell cathode achieve superior dynamic and static stabilities despite the large amount of active material and lean electrolyte (8 μL mg^{-1}). The core-shell cathodes exhibit a high areal capacity and energy density of, respectively, 14 mA h cm^{-2} and 27 mW h cm^{-2}. During resting, the cells show a long shelf-life of over one month and a low self-discharge effect with a capacity-fade rate of only 0.25% per day.

Results and discussion

We design the core-shell carbon substrate by using conductive carbon nanofibers (CNFs) via a phase-inversion method (Fig. 1a). This fabrication method enables the formation of a porous internal region, as shown in the scanning electron microscopy (SEM) image (Fig. 1b). Large open pores are observed inside the substrate. The diameter of these large open pores is in the range of tens to hundreds of μm. As we look through the large open pores, the inner porous network shows high porosity and tortuosity. However, the microstructure of the external region is quite different. The SEM inspection from the dense external region displays tightly entangled CNF shell network. It is hard to find open pores or porous structure (Fig. 1c). The corresponding cross-sectional SEM inspection (Fig. S1) demonstrates that the core-shell CNF substrate has the internal porous spaces for hosting the active material as a sulfur core. Outside of the core, the interweaving CNF shell network provides the encapsulated sulfur with high conductivity and deters the active material loss during cycling.

We then add polysulfide catholyte into the internal porous region of the core-shell CNF substrate to form the core-shell cathode, which absorbs a high amount of active material (Fig. 1d). To verify such a design, we analyze the microstructure of the internal and external regions of a freshly-made core-shell cathode. Fig. 1e shows the SEM images of the internal region of the cathode, where the CNF porous network encapsulates a high amount of sulfur. More interestingly, we find the active material is accommodated within the large open pores. Together with the strong sulfur signals detected in the elemental mapping results (Fig. S2), we provide solid evidence proving the formation of the active material core at the internal region of the core-shell cathode. The microstructural observation from the external region shows no obvious sulfur species on the tightly connected CNF shell network (Fig. 1f). The corresponding elemental mapping result reconfirms this by showing weak sulfur signals (Fig. S3). These indicate that the CNF shell could block the free migration of polysulfides.

According to the microstructural analysis and the substrate design, we could comment the three major advantages brought about by this core-shell CNF substrate:

(1) Distinguishable internal/external morphologies: the core-shell CNF substrate has distinct internal and external regions, which facilitate the electrochemical performance of the cell in two different ways. The internal porous core accommodates and absorbs a large amount of sulfur, benefiting the high sulfur loading.[2,3] The external dense shell consists of tightly entangled CNF network, which increases the electronic conductivity of the cathode and seals the active material within the core-shell CNF substrate.[13,14]

(2) Integrated structure: the CNF substrate is self-assembled with the woven CNF/Poly(vinylidiene fluoride-hexafluoropropylene) (PVDF-HFP) network to form a three-dimensional structure during the phase separation spontaneously.[22] Thus, the internal porous core for hosting sulfur integrates inherently with the external shell, showing good structural integrity. The connected CNF network forms interconnected channels, which supply smooth ion transport and thereby reduce the E/S ratio.[17]

(3) Continuous conductive network: The integrated CNF network creates a continuous conductive network from the external shell to the internal core. Thus, our high-loading sulfur core has CNFs fully wrapping the active material for improving

This journal is © The Royal Society of Chemistry 20xx

Please do not adjust margins

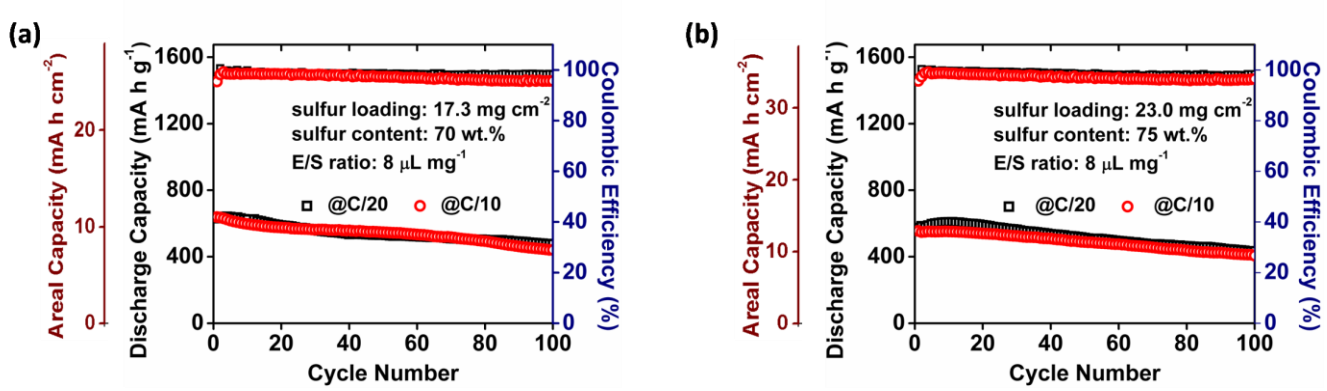

Fig. 2. Cycling performance of the core-shell cathodes with sulfur loadings of (a) 17.3 mg cm^{-2} and (b) 23.0 mg cm^{-2}.

the reaction kinetics. The woven CNF network also increases the tortuosity of the internal porous space. These hinder the leakage of polysulfides[6,12] and help buffer the volume change during the lithiation/delithiation reaction.[5,13,15]

Therefore, we are allowed to seal a high amount of sulfur in the cathode, achieving a high sulfur loading and content of, respectively, 17.3 mg cm^{-2} and 70 wt.%. Fig. 2a shows the electrochemical performances of the high-loading core-shell cathodes cycled at a low E/S ratio of 8 μL mg^{-1}. At C/20 and C/10 rates, the cells attain peak capacities of, respectively, 641 and 639 mA h g^{-1}, corresponding to high areal capacities of 11.1 and 11.0 mA h cm^{-2}. The resulting energy densities are 21.2 and 20.4 mW h cm^{-2} (Fig. S4). After 100 cycles, the cells keep high capacity retentions of 75% and 70% at, respectively, C/20 and C/10 rates. The effective capacity and energy density of our cathodes clearly outperform the strict benchmarks suggested for developing advanced high-loading cathodes, which need an areal capacity and an energy density of over, respectively, 4.0 mA h cm^{-2} and 10.1 mW h cm^{-2}.[2-4]

To challenge the capability of our cathode design in hosting a high amount of sulfur, we simultaneously increase the sulfur loading and sulfur content to, respectively, 23.0 mg cm^{-2} and 75 wt.%, which are relatively high among the cell-fabrication parameters used in high-loading cathodes reported in the literature (Table S1). At a C/20 rate, the cell delivers a peak areal capacity of 14.0 mA h cm^{-2}, corresponding to a high energy density of 27.0 mW h cm^{-2} (Fig. S5), and maintains 71% of the original capacity after 100 cycles (Fig. 2b). At an even higher C/10 rate, the cell offers a peak areal capacity of 12.8 mA h cm^{-2} and a high capacity retention of 73% after 100 cycles. A high Coulombic efficiency of above 97% attained by these cells indicates the suppression of the fast consumption of electrolyte. At a lean electrolyte condition, the excellent cycling performance of the cathodes with an even higher sulphur loading demonstrates that our core-shell cathode blocks the severe polysulfide diffusion and provides effective reaction capability to the encapsulated active material. These positive features result in an enhanced the cycle stability of the high-loading sulfur cathodes at both low C/20 and high C/10 rates.[4-6,10] Considering the critical parameters, with high sulfur loading, high sulfur content, and lean electrolyte, this core-shell strategy increases the practicality of lithium-sulfur cells.

Fig.3a gives the cyclic voltammetry (CV) curves of the core-shell cathode with a sulfur loading of 17.3 mg cm^{-2}. The cell is charged to 3.0 V in the initial cycle. During this oxidation process, the active material (Li_2S_6) is converted to sulfur (S_8). In the following cycles, the multi-step reactions of sulfur result in two cathodic peaks in the reduction process. The first peak at 2.23 V is assigned to the transformation of cyclo-octasulfur (S_8) to lithium polysulfides (Li_2S_n, 4≤ n≤8). The second peak at 1.92 V corresponds to the conversion of lithium polysulfides to lithium sulfides (Li_2S_2/Li_2S). In the oxidation scan, one overlapping anodic peak resulting from the conversion of sulfides and polysulfides into sulfur is seen.[7,8] The CV curves show no apparent degradations of the redox peak currents

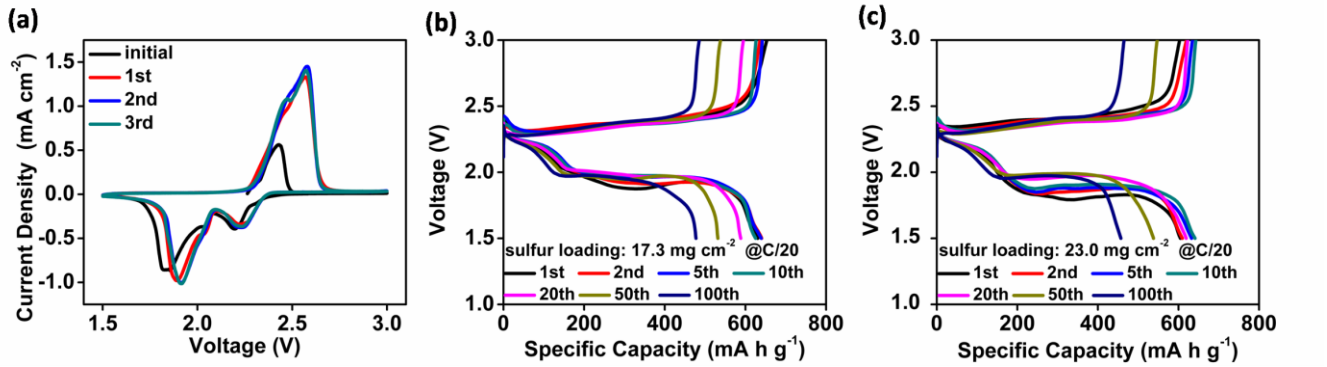

Fig. 3. (a) CV curves, and voltage profiles of the core-shell cathodes with sulfur loadings of (b) 17.3 mg cm^{-2} and (c) 23.0 mg cm^{-2}.

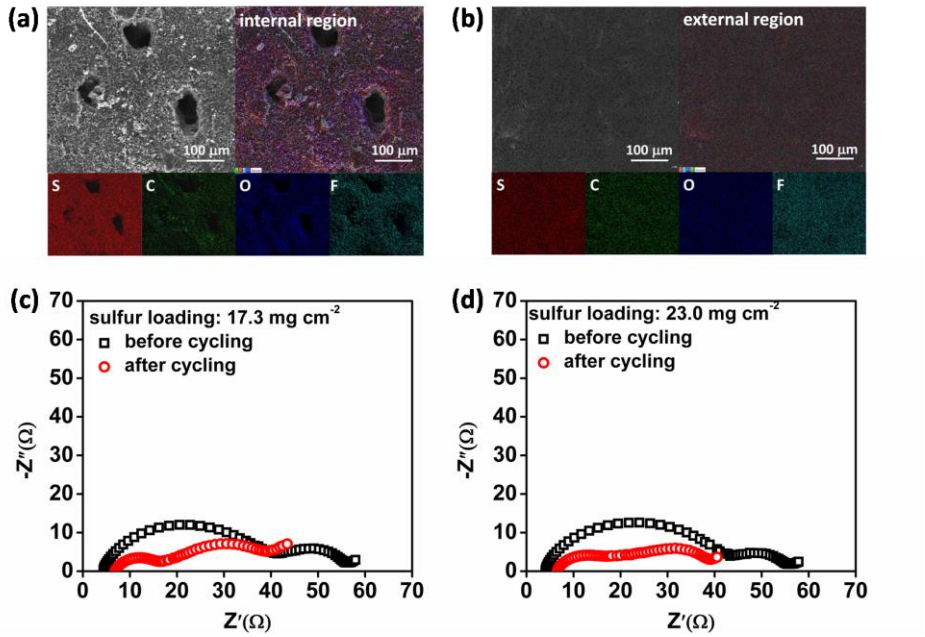

Fig. 4. Microstructure analysis of the (a) internal and (b) external regions of the core-shell cathodes after 100 cycles. Electrochemical impedance spectra of the core-shell cathodes with sulfur loadings of (c) 17.3 mg $cm^{-2}$and (d) 23.0 mg cm^{-2} before and after cycling.

and potentials, indicating a good reversibility of the core-shell cathode.[8,9] The CV curves of the core-shell cathode with a sulfur loading of 23.0 mg cm^{-2} (Fig. S6) show similar results.

Fig.3b,c illustrates the charge and discharge curves of the cathodes with sulfur loadings of 17.3 and 23.0 mg cm^{-2}. The voltage profiles contain two discharge plateaus and one continuous charge plateau, which agree with, respectively, the cathodic and anodic peaks in the CV analysis. The initial discharge curves show a high polarization potential, whereas, the voltage hysteresis decreases gradually in the subsequent cycles. This is because the large pores inside the core-shell CNF substrate easily absorb a high amount of active material. The encapsulated sulfur inescapably aggregates as clusters during cathode preparation so that we can find the agglomeration in the internal porous core (Fig. 1e). However, after repeatedly cycling for a few cycles, the redistributed active material attains better uniformity and has closer contact with the internal conductive CNF matrix, leading to a decrease in the cell polarization.[18,23] The SEM images in Fig.4a affirm the more uniform distribution of sulphur in the internal porous core after cycling. Correspondingly, Fig.4b confirms the relocation of sulphur occurring only within the core region by showing no detectable re-deposition of sulphur species or structural damage in the shell region. The result of these are reflected in the reduction in the total resistance of the cells, as proved by the electrochemical impedance analysis (Fig.4c,d and Fig.

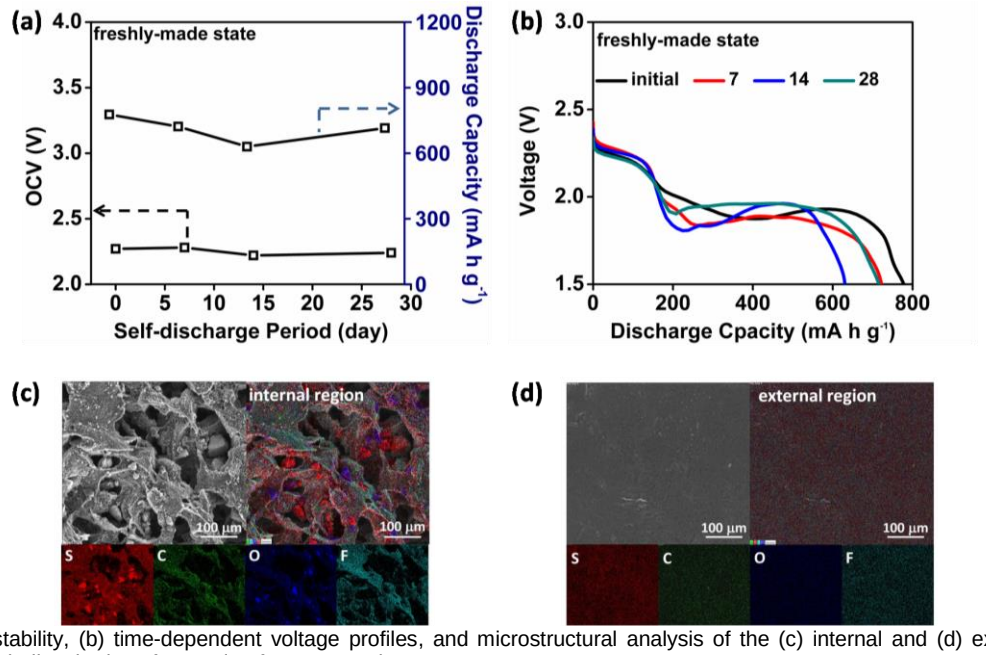

Fig. 5. (a) Static stability, (b) time-dependent voltage profiles, and microstructural analysis of the (c) internal and (d) external regions of freshly-made core-shell cathodes after resting for one month.

This journal is © The Royal Society of Chemistry 20xx

Please do not adjust margins

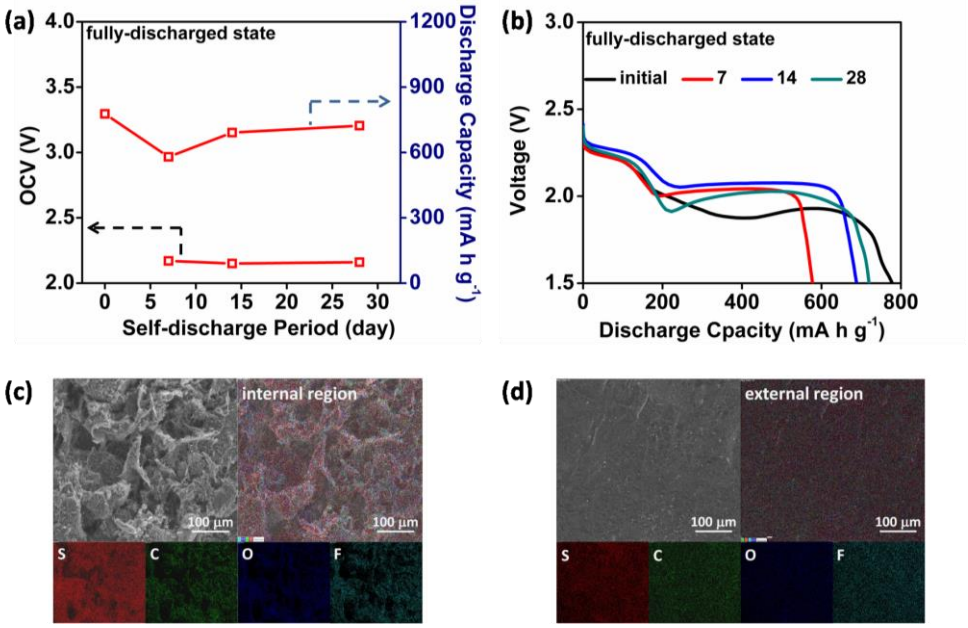

Fig. 6. (a) Static stability, (b) time-dependent voltage profiles, and microstructural analysis of the (c) internal and (d) external regions of fully-discharged core-shell cathodes after resting for one month.

S7).[15,16] This is likely associated with the better accessibility of the sealed active material by electronic conduction, which leads to fast charge transfer.[23] The reduced polarization and the subsequent long cycle stability could also be found in the cells cycled at high C/10 rate, as summarized in Fig. S8.

Moreover, we demonstrate our core-shell cathodes with high static stability, which overcomes the fast self-discharge encountered with lithium-sulfur batteries.[24] We record the changes in the open-circuit voltage (OCV) values and the charge-storage capacities of the core-shell cathodes during a one-month rest period. Fig.5a reveals the performances of the cells resting at freshly-made state. The freshly-made cells display only a very slight OCV drop from 2.27 V to 2.24 V. Theoretically, the highly active polysulfides in the freshly-made cells would dissolve in the electrolyte and intensively diffuse toward the anode. The resulting loss of active material and the corrosion of lithium-metal anode cause the OCV drop as reported in the literature.[24,25] Thus, in our core-shell cathodes, the low OCV drop indicates a suppressed polysulfide diffusion. Additionally, our sulfur loading is as high as 17.3 mg cm^{-2}, meaning quite a large amount of active material is stored in the CNF shell. Therefore, the ability of the core-shell cathode to accommodate the active material is proved. As a result, the freshly-made cells achieve a high capacity retention of 92% after resting for one month.

The enhanced stability is further proved by the time-dependent voltage profiles. In Fig.5b, the voltage profiles keep two distinct discharge plateaus after resting for one, two, and four weeks. However, in conventional cells, the irreversible polysulfide loss and limited redox reactions cause the declining of discharge curves, especially, the collapse of the upper discharge plateau.[24,25] Thus, the intact discharge plateaus demonstrate strong polysulfide retention and high reaction capability of our core-shell cathodes. Additionally, Fig.5c suggests the strong elemental sulfur signals at the internal region of the cathode after resting for one month. In comparison, the external region of the rested cathodes shows weaker sulfur signals (Fig.5d). This verifies the suppressed active material loss of our cathode during resting at freshly-made state.

The improved static stability of the core-shell cathodes is also demonstrated by the cells rested at the fully-discharged state. The fully-discharged cells exhibit almost constant OCV values of 2.17 – 2.15 V and low capacity-fade rate of only 0.25% per day after resting for one month (Fig.6a). It is known that the conventional cells encounter the re-deposition of insulating Li_2S_2/Li_2S at fully-discharged state. During resting, the discharge products would gradually form inactive area in the cathode and reduce the electrochemical accessibility.[4,5,10] Thus, the stable OCV values and high capacity retention prove the high reaction ability of our cathodes when resting at the fully-discharged state.

The fully-discharged cells resting for different periods still keep extant upper and lower discharge plateaus (Fig.6b). The remaining representative discharge curves confirm the uninterrupted electron/ion pathways and the high reversible utilization of active material after resting.[21] Furthermore, after resting, the lower discharge plateaus of all fully-discharged cells increase as compared with the discharge curve collected from the un-rested cells. This is because the added sulfur might already make certain rearrangement toward the electrochemically favorable sites in the core region during the initial discharge process.[18,23] As an evidence, the microstructural analysis indicates uniform and strong elemental sulfur signals at the internal region (Fig.6c), demonstrating the limited accumulation of insulting Li_2S_2/Li_2S during resting. Moreover, the weak sulfur signals at the external region illustrate the core-shell structure of our cathodes (Fig.6d).

Experimental

Preparation of the core-shell CNF substrate: 5.0 wt.% Poly(vinylidiene fluoride-hexafluoropropylene) (PVDF-HFP, Sigma-Aldrich) was dissolved in N-methylpyrrolidone (NMP, Sigma-Aldrich) at 50 °C as the precursor solution. Then, 9.5 wt.% carbon nanofibers (CNFs, PR-19-XT-HHT) were added to the precursor solution under vigorous stirring to form a uniform CNF/PVDF-HFP slurry. The resulting slurry was coated onto a piece of glass to form a CNF/PVDF-HFP thin film, which was immersed in distilled water. During the immersion process, the exchange of NMP (solvent for PVDF-HFP) in the slurry with distilled water (non-solvent for PVDF-HFP) results in a phase separation. This step results in the fabrication of the integrated porous core and dense shell of the CNF substrate.[27] After resting for 10 minutes, the CNF/PVDF-HFP thin film was able to be peeled off from the glass. The free-standing thin filmwas dried in a vacuum oven at 50 °C for 24 h. The resulting CNF/PVDF-HFP thin film spontaneously formed an internal porous region and an external dense CNF shell network together.

Material characterization: Microstructure of the core-shell CNF substrate and the morphological and elemental changes of the resulting core-shell cathodes were inspected with a field emission scanning electron microscope (FE-SEM,Quanta 600, FEI) and an energy dispersive X-ray spectrometer (EDX) for the collection of the elemental signals (*i.e.*, elemental sulfur, carbon, fluorine, and oxygen). Two inspection conditions were considered, which included the cathode morphologies before and after cycling as well as before and after resting.

Electrochemical cell assembly: The core-shell CNF substrate was cut into round pieces with an area of 2.0 cm^2 and was used as the cathode substrate. The core-shell cathode was prepared by adding catholyte into the internal porous region of two pieces of CNF substrates and aligning the filled internal region together inside an argon-filled glovebox. The catholyte consists of Li_2S_6 polysulfides in the electrolyte that contained 1.85 M LiTFSI lithium salt and 0.2 M$LiNO_3$lithium salt in 1, 2-dimethoxymethane (DME)/1, 3-dioxolane (DOL) (v/v=1/1).Except $LiNO_3$ from Acros Organics, all other chemicals used for preparing the catholyte and electrolyte were from Sigma-Aldish. The mass of sulfur was calculated based on the amount of the catholyte. The sulfur loadings of the resulting core-shell cathodes were 17.3 and 23.0 mg cm^{-2}, corresponding to high sulfur contents of, respectively, 70 wt.% and 75 wt.% with the consideration of the mass of sulfur and the core-shell CNF substrate. The coin cells were assembled with the obtained core-shell cathode, lithium foil as the anode, and the Celgard 2500 membrane as separator. The electrolyte/sulfur (E/S) ratio of the resulting cell was 8 μL mg^{-1} based on the total amount of electrolyte in the cell and total mass of sulfur. No metal current collector was used because aluminum foil was reported to be corroded by polysulfides.[26] The charge-discharge measurements were carried out with a battery cycler (Arbin Instruments) at different cycling rates over the voltage range of 1.5 – 3.0 V (vs Li/Li^+). The discharge capacity was calculated based on the mass of sulfur and the theoretical capacity. The areal capacity was calculated by considering the discharge capacity obtained and the sulfur loading in the cell. According to this, we integrated the areal capacity with the operating voltage to get the areal energy density. Specifically, the units of discharge capacity, sulfur loading, discharge voltage, areal capacity, and areal energy density are, respectively, mA h g^{-1}, mg cm^{-2}, V, mA h cm^{-2}, and mW h cm^{-2}. The cyclic voltammetry (CV) measurements were made with a universal potentiostat (VoltaLab PGZ 402,Radiometer Analytical) at 0.01 mV s^{-1} rate. The electrochemical impedance of the cells at the freshly-made (before cycling) and fully-discharged states (after 100 cycles) was evaluated with a frequency analyzer Solartron 1260/1287 and the frequency was from 0.1 Hz to 1 M Hz with an applied voltage amplitude of 5 mV. To test the self-discharge behavior, the changes of open-circuit voltage (OCV) values and charge-storage capacities were recorded and analyzed. Both freshly-made and fully-discharged cells were tested after resting for one, two, and four weeks.

Conclusions

In conclusion, we have developed a core-shell CNF substrate with an internal porous region and an external CNF shell network for, respectively, accommodating and encapsulating the active material. The resulting core-shell cathodes simultaneously attain a high sulfur loading and content of, respectively, 23.0 mg cm^{-2} and 75 wt.%. With a low E/S ratio of 8μL mg^{-1}, the core-shell cathodes exhibit a high areal capacity and energy density of, respectively, 14.0 mA h cm^{-2} and 27.0 mW h $cm^{-2}$and achieve a high capacity retention of 71% after long cycle. Furthermore, the cells display a long shelf-life of one month with a high capacity retention of above 92%. These enhanced electrochemical performances during cycling and resting result from the integrated core-shell architecture of the CNF substrate. Through the phase inversion process, the internal core region has the CNFs backbone and network as the fast electron and ion pathways, which effectively overcome the sluggish reaction kinetics of high-loading sulfur cathodes at lean electrolyte conduction.

Conflicts of interest

There are no conflicts to declare.

Acknowledgements

This work was supported by the U.S. Department of Energy, Office of Basic Energy Sciences, Division of Materials Science and Engineering under award number DE-SC0005397. One of the authors (R.Y.) thanks the China Scholarship Council (Grant No. 201706340107) for the award of a fellowship.

This journal is © The Royal Society of Chemistry 20xx

Please do not adjust margins

References

1 A.Manthiram, Y.Fu,S.-H.Chung, C.Zu, Y.-S.Su, *Chem. Rev.*, 2014, **114**, 11751.
2 S.-H.Chung, C.-H.Chang, A.Manthiram, *Adv. Funct. Mater.*,2018,**28**, 1801188.
3 H.-J.Peng, J.-Q.Huang, X.-B.Cheng, Q.Zhang, *Adv. Energy Mater.*,2017, **7**, 1700260.
4 R.Fang, S.Zhao, Z.Sun, D.-W.Wang, H.-M.Cheng, F.Li, *Adv. Mater.*, 2017, **29**, 1606823.
5 Z.-L.Xu, J.-K.Kim, K.Kang, *Nano Today*,2018, **19**, 84.
6 H.Shi, W.Lv, C.Zhang, D.-W.Wang, G.Ling, Y.He, F.Kang, Q.-H.Yang, *Adv. Funct. Mater.*, 2018, 1800508.
7 L.Xiao,Y. Cao, J.Xiao, B.Schwenzer, M. H.Englhard, L. V.Saraf, Z.Nie, G. J.Exarhos, J.Liu, *Adv. Mater.*,2012,**24**, 1176.
8 L.-X.Miao, W.-K.Wang, A.-B.Wang, K.-G.Yuan, Y.-S.Yang, *J. Mater. Chem. A*,2013, **1**, 11659.
9 G.-C.Li, G.-R.Li, S.-H.Ye, X.-P.Gao, *Adv. Energy Mater.*, 2012, **2**, 1238.
10 F.Wu, J.Chen, R.Chen,S. Wu, L.Li, *J. Phys. Chem. C*,2011, **115**, 6057.
11 S.Li, T.Mou, G.Ren, J.Warzywoda, B.Wang, Z.Fan, *ACS Energy Lett.*, 2016, **1**, 481.
12 M.Xiao, M.Huang, S.Zeng, D.Han, S.Wang, L.Sun, Y.Meng, *RSC Adv.*,2013, **3**, 4914.
13 Q.Li, Z.Zhang, Z.Guo, Y.Lai, K.Zhang, J.Li, *Carbon*, 2014, **78**, 1.
14 C.Nan, Z.Lin, H.Liao, M.-K.Song, Y.Li, E. J. Cairns, *J. Am. Chem. Soc.*,2014, **136**, 4659.
15 H.Xu, Y.Deng, Z.Shi, Y.Qian, Y.Meng, G.Chen, *J. Mater. Chem. A*, 2013, **1**, 15142.
16 B.Ding, L.Shen, G.Xu, P.Nie, X.Zhang, *Electrochim. Acta*,2013, **107**, 78.
17 S.-H.Chung, A.Manthiram, *Adv. Mater.*, 2018, **30**, 1705951.
18 F.Zeng, A.Wang, W.Wang, Z.Jin, Y.-S.Yang, *J. Mater. Chem. A*,2017, **5**, 12879.
19 M.Li, Y.Zhang, F.Hassan, W.Ahn, X.Wang, W. W.Liu, G.Jiang, Z.Chen, *J. Mater. Chem. A*,2017, **5**, 21435.
20 Z.Liu, X.Zheng, N.Yuan, J.Ding, *J. Mater. Chem. A*,2017, **5**, 942.
21 S.-H.Chung, C.-H.Chang, A.Manthiram, *Energy Environ. Sci.*, 2016, **9**, 3188.
22 X.Yang, Y.Chen,M. Wang, H.Zhang, X.Li, H.Zhang, *Adv. Funct. Mater.*,2016, **26**, 8427.
23 N. A.Canas, K.Hirose, B.Pascucci,N. Wagner, *Electrochim. Acta*, 2013, **97**, 42.
24 S.-H.Chung, A.Manthiram, *ACS Energy Lett.*,2017, **2**, 1056.
25 Y. V.Mikhaylik, J. R.Akridge, *J. Electrochem. Soc.*, 2004, **151**, A1969.
26 H.-J.Peng, W.-T.Xu, L.Zhu, D.-W.Wang, J.-Q.Huang, X.-B.Cheng, Z.Yuan,F.Wei, Q.Zhang, *Adv. Funct.Mater.*,2016, **26**, 6351.
27 F. Liu, N. A. Hashim, Y. Liu, M. R. M. Abed, K. Li, *J. Membrane Sci.*, 2011, **375**, 1.

Graphic Abstract

A Core-shell Cathode Substrate for Developing High-loading, High-performance Lithium-sulfur Batteries

Ran Yu,[a,b] Sheng-Heng Chung,[a] Chun-Hua Chen,[*,b] and Arumugam Manthiram[*,a]
[a]Materials Science and Engineering Program & Texas Materials Institute
University of Texas at Austin, Austin, Texas 78712, United States
[b]CAS Key Laboratory of Materials for Energy Conversions, Department of Materials Science and Engineering & Collaborative Innovation Center of Suzhou Nano Science and Technology, University of Science and Technology of China, Anhui Hefei 230026, China

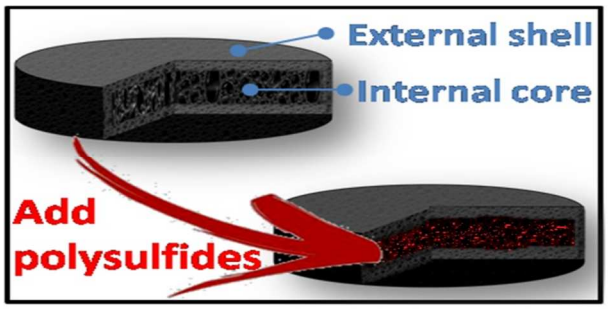

The internal porous core and external dense shell of the three-dimensional cathode substrate, respectively, accommodate and encapsulate a large amount of active material.